Toxicology Reports 7 (2020) 637–648

Contents lists available at ScienceDirect

Toxicology Reports

journal homepage: www.elsevier.com/locate/toxrep

Cadmium sulfide-induced toxicity in the cortex and cerebellum: *In vitro* and *in vivo* studies

Atefeh Varmazyari[a], Ali Taghizadehghalehjoughi[a,b,*], Cigdem Sevim[b], Ozlem Baris[a], Gizem Eser[c], Serkan Yildirim[d], Ahmet Hacimuftuoglu[e], Aleksandra Buha[f], David R. Wallace[g], Aristidis Tsatsakis[h], Michael Aschner[i], Yaroslav Mezhuev[j]

[a] Department of Nanoscience and Nanoengineering, Institute of Naturel and Applied Sciences, Ataturk University, Postal Code 25240, Erzurum, Turkey
[b] Department of Pharmacology and Toxicology, Faculty of Veterinary Science, Ataturk University, Postal code 25240, Erzurum, Turkey
[c] Vocational School of Veterinary Laboratory Assistant Program, Igdir University, Postal Code 76103, Igdir, Turkey
[d] Department of Pathology, Faculty of Medicine Science, Ataturk University, Postal Code 25240, Erzurum, Turkey
[e] Department of Pharmacology, Faculty of Medicine Science, Atatürk University, Postal Code 25240, Erzurum, Turkey
[f] Department of Toxicology "Akademik Danilo Soldatović", Faculty of Pharmacy, University of Belgrade, Postal Code 11000, Belgrade, Serbia
[g] Department of Pharmacology, School of Biomedical Sciences, Oklahoma State University Center for Health Sciences, Postal Code 74107, Tulsa, OK, USA
[h] Department of Toxicology & Forensic Sciences, Faculty Medicine, University of Crete, Postal Code 74100, Heraklion, Greece
[i] Department of Molecular Pharmacology, Albert Einstein College of Medicine, Bronx, NY 10463, USA
[j] Center of Biomaterials, D. Mendeleev University of Chemical Technology of Russia, Postal Code 125047, Moscow, Russia

ARTICLE INFO

Keywords:
CdS
Cerebellum neuron
Green synthesis
Neurotoxicity
Quantum dots

ABSTRACT

Living organisms have an innate ability to regulate the synthesis of inorganic materials, such as bones and teeth in humans. Cadmium sulfide (CdS) can be utilized as a quantum dot that functions as a unique light-emitting semiconductor nanocrystal. The increased use in CdS has led to an increased inhalation and ingestion rate of CdS by humans which requires a broader appreciation for the acute and chronic toxicity of CdS. We investigated the toxic effects of CdS on cerebellar cell cultures and rat brain. We employed a 'green synthesis' biosynthesis process to obtain biocompatible material that can be used in living organisms, such as *Viridibacillus arenosi* K64. Nanocrystal formation was initiated by adding $CdCl_2$ (1 mM) to the cell cultures. Our *in vitro* results established that increased concentrations of CdS (0.1 μg/mL) lead to decreased cell viability as assessed using 3-[4,5-dimethylthiazole-2-yl]-2,5-diphenyltetrazolium bromide (MTT), total antioxidant capacity (TAC), and total oxidant status (TOS). The *in vivo* studies showed that exposure to CdS (1 mg/kg) glial fibrillary acidic protein (GFAP) and 8-hydroxy-2' -deoxyguanosine (8-OHdG) were increased. Collectively, we describe a model system that addresses the process from the synthesis to the neurotoxicity assessment for CdS both *in vitro* and *in vivo*. These data will be beneficial in establishing a more comprehensive pathway for the understanding of quantum dot-induced neurotoxicity.

1. Introduction

Currently, the use of nanoparticles (NPs) in medicine is rapidly expanding for diagnostic or treatment purposes [1–3]. The unique properties of NPs include their small size, wide surface area, and their use as a vehicle for the transport of other compounds [4,5]. Nanoparticles have been successfully used in the diagnosis of cancer, blood vessel visualization and single cell diagnostics [6–9]. Further, they can be utilized in the treatment of malignant diseases and neuronal illnesses, given their ability to deliver genes to single cells [10,11]. Over the last decade, the use of NPs in the medical field has grown significantly, and as the technology employed in NPs synthesis will continue to improve, their medical applications will continue to expand into new areas of therapy [11]. Nonetheless, the full understanding of their toxicity has yet to be addressed).

Cadmium (Cd) is a heavy metal that occurs naturally in the earth's crust and is a primary industrial and environmental pollutant, and a significant anthropogenic toxicant [12–14]). It is also present in various food items [15], and its toxicity has been widely documented in both humans and animal models [16,15,12,17,18]. Cd exists in an inorganic

* Corresponding author at: Department of Nanoscience and Nanoengineering, Institute of Naturel and Applied Sciences, Ataturk University, Postal Code 25240, Erzurum, Turkey.
E-mail address: alitgzd@gmail.com (A. Taghizadehghalehjoughi).

https://doi.org/10.1016/j.toxrep.2020.04.011
Received 28 July 2019; Received in revised form 17 April 2020; Accepted 21 April 2020
Available online 06 May 2020

state as Cd sulfide (CdS), which is found as an impurity in zinc ores and as such, is a waste product of zinc mining [19]. CdS has been used as a semiconductor that has already found a use for the formation of quantum dots but has not exhausted the potential for further use in the size of "Nano" [20]. Li et al. [21] reported that the toxicity of the pure Cd metal is higher than that of CdS. CdS has been used to construct unique light-emitting semiconductor nanocrystals and it is also widely used as a color pigment in various industrial products. Recently, the efficacy of CdS nanoparticles has been explored as a drug delivery system or carrier to promote drug delivery to desired sites [22–25]. Increasing the functional area of nanoparticles may increase the risk of toxicity, especially in a biological system [4,12]. Modlitbova et al. demonstrated that the size of CdS particles is directly related to the toxicity exhibited by the particle [26,27]. A significant challenge confronting research in the field of nanoparticle synthesis is the growing need to develop reliable, non-toxic, clean, eco-friendly, and green experimental protocols [28–30]. One synthesis option that meets the needs listed above is the use of natural processes, such as the use of enzymes, vitamins, polysaccharides, biodegradable polymers, microorganisms, and biological systems for the synthesis of NPs.

Our focus has been to develop a method that will provide a controlled and up-scalable process for the biosynthesis of monodispersed and highly stable NPs. Thus, a wide range of bacterial species has been used in green nanotechnology for the synthesis of NPs utilizing gold, silver, platinum, palladium, titanium, titanium dioxide, magnetite, and cadmium sulfide among other elements [31,32]. Little evidence exists regarding the "green synthesis" of CdS by bacteria. Hence, it is essential to widen the range of biosynthesized CdS NPs toxicity investigations.

Changes in neuronal function can impact our posture, balance, coordination, and speech. Since CdS easily cross the blood-brain barrier (BBB) it has been used to visualize brain blood vessels [33], and tumors [34,35]. CdS has also been studied for the treatment of neurodegenerative diseases such as Parkinson's disease [36] and Alzheimer's disease [37]. Cell viability, antioxidant capacity, and oxidant status are some of the parameters that need to be further investigated in response to CdS exposures. In the present study, we evaluated the neurotoxicity of various concentrations and doses of biosynthesized CdS both *in vitro* and *in vivo* systems, respectively.

2. Methods

2.1. Biosynthesis of CdS NPs

2.1.1. Chemicals and reagents

All media (Dulbecco Modified Eagle's (DMEM), Neurobasal (NBM), Roswell Park Memorial Institute (RPMI 1640), and supplements, Fetal Calf Serum (FCS), phosphate buffer solution (PBS); antibiotic/antimycotic solution (100×), L-glutamine, and trypsin–EDTA were obtained from Sigma-Aldrich (St. Louis, MO, USA).

2.1.2. Bacteria and biosynthesis of CdS NPs

The biosynthesis process is designed to obtain highly biocompatible material that can be used in living organisms. *Viridibacillus arenosi* K64 (GenBank Accession Number: KR873397), were obtained from Atatürk University East Anatolia High Technology Application and Research Center (DAYTAM) culture collection.

The cultures were grown overnight in an incubator (120 rpm/min, 32 °C) inoculated with 100 ml LB (Luria Bertani) broth medium (yeast extract 5.0 g/L; peptone 10.0 g/l; NaCl 10.0 g/l) and left to incubate. The culture on LB broth medium was centrifuged at 6000 rpm at 20 °C for 10 min. The supernatant was allowed to incubate for 36 h in culture on a shaker (120 rpm, 32 °C). After 36 h, the culture was diluted by adding an equal volume of sterile and fresh LB broth. The culture was returned to the shaker for another 24 h (120 rpm, 32 °C). At the end of the incubation, the culture was re-centrifuged and 20 ml of 0.25 M $CdCl_2$ and 5 ml of 0.5 M Na_2S were added in the supernatant which was

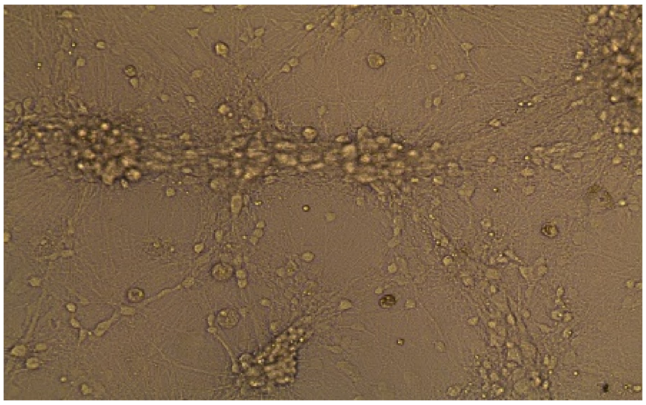

Fig. 1. Harvested cell line (×10): Cerebellum neuron cells.

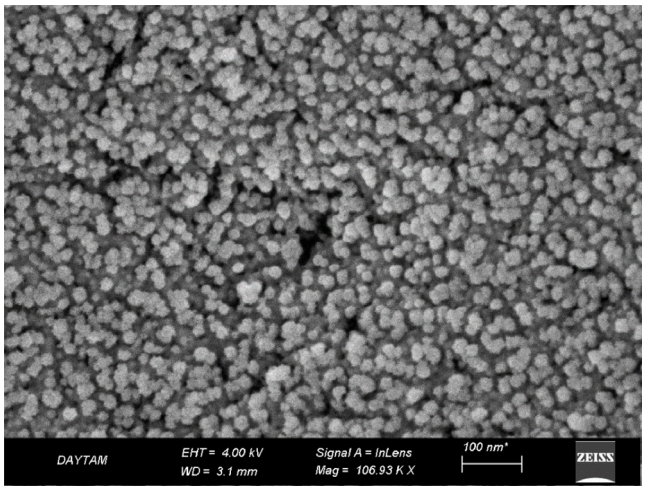

Fig. 2. Scanning electron microscopy (SEM) images of CdS NPs shapes and sizes. (EHT = 4.00 kV).

incubated at 60 °C for 10–20 min until a yellow-white color was observed. The resulting NPs were allowed to stand at room temperature (22 − 25 °C) for 24 h to obtain the final usable NPs [38,39].

$$CdCl_2 + Na_2S \rightarrow CdS + 2NaCl$$

(seed crystal)

$$CdCl_2 + S^{2-} \rightarrow CdS + 2Cl^-$$

(bacterial origin)

2.1.3. Isolation and purification of CdS nanoparticles

After 24 h at room temperature, the synthesized solution was transferred to a 50 ml tube and centrifuged at 10,000 rpm at 20 °C for 10 min. The precipitate containing CdS was washed with n-hexane, methanol, and ddH_2O, respectively. After each wash, the wash solutions were removed by repeating the centrifugation step of 10,000 rpm at 20 °C for 10 min [40–43]. The resulting precipitate was dried for 24 h at 60 °C before characterization.

2.1.4. Characterization of CdS nanoparticles

The biosynthesized CdS nanoparticles were characterized by X-ray powder diffraction (XRD, PANalytical Empyrean Inspect S50, USA), scanning electron microscope (SEM) (Zeiss Sigma 300, Germany). All analyses were made through the purchase of services from Atatürk University DAYTAM.

2.1.5. In vitro studies

Cerebellum cell cultures were obtained from the Department of Medical Pharmacology at Ataturk University (Erzurum, Turkey)

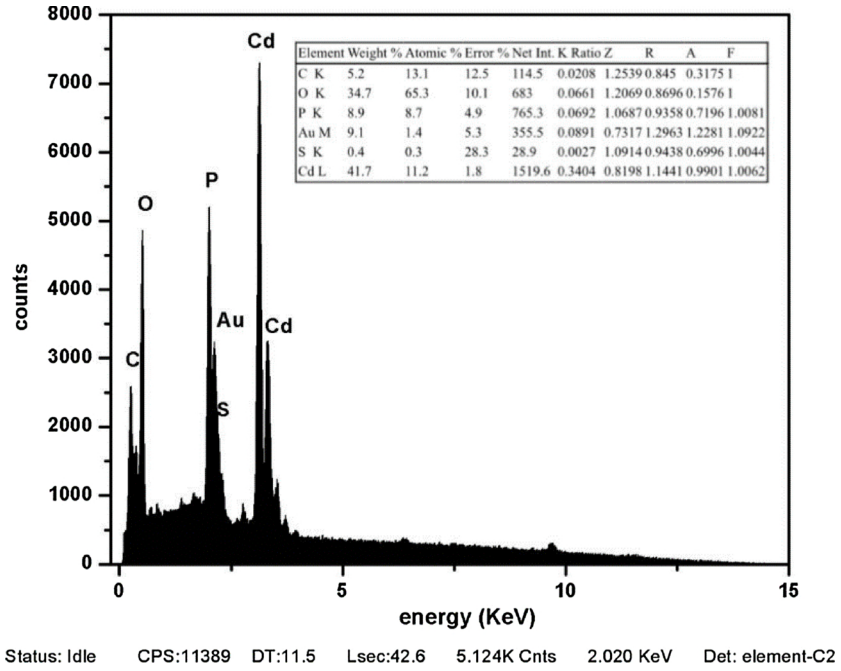

Fig. 3. EDX and elemental mapping of CdS nanoparticles. The estimated band gap value for CdS is 2.02 eV.

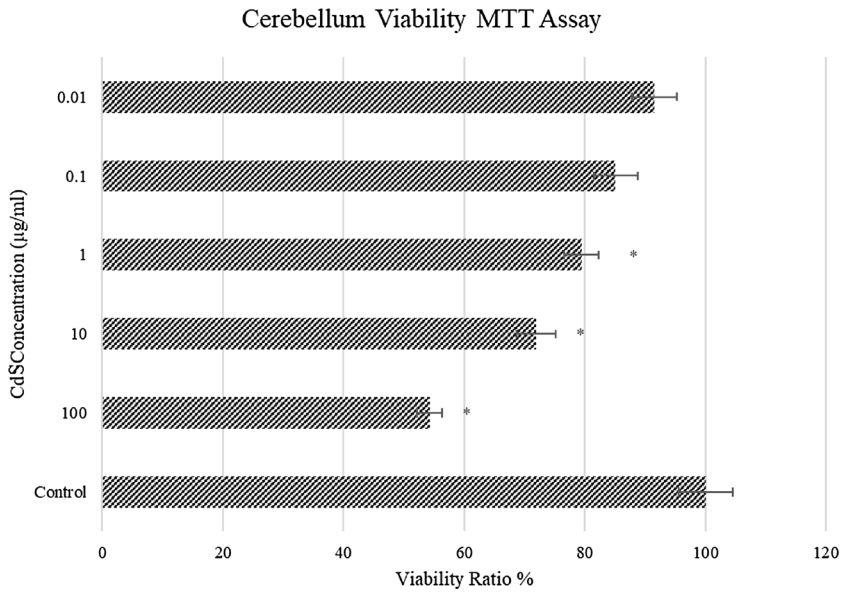

Fig. 4. *In vitro* viability ratio of CdS (0.01 – 100 µg/mL) on cerebellum neuron cells (n = 6/group). * Significant differences at $P < 0.05$ compared to control group; ** Significant differences at $P < 0.001$ compared to control group.

(Fig. 1). The cells were thawed and briefly centrifuged to form a pellet. The pellet was resuspended in growth media, and the cells (1×10^5 cells/mL) were seeded into a 48-well culture plate. The cells were treated with increasing concentrations of CdS (0.01–100 µg/ml) and incubated for 24 h (5% CO_2; 37 °C). As a control, 150 µl NBM (Gibco, sigma, USA) only was added to one set of wells for 24 h. Following 24 h incubation, cell viability was determined using the commercially available MTT assay (Cayman Chemical, MI, USA). Briefly, 10 µl of MTT reagent was added to each well, and incubated (5% CO_2; 3 °C) for 4 h. After incubation, the media was removed and replaced with 100 µl of dimethyl sulfoxide (DMSO). The optical density (OD) was determined at 570 nm using Multiskan™ GO Microplate Spectrophotometer reader (Thermo Scientific, Canada), and the cell viability (%) was calculated. TAC and TOS status were investigated with commercially available kits (Rel assay, Turkey) that were used according to the manufacturer's suggested procedure. The evaluation was made spectrophotometrically (Multiskan™ GO Microplate Spectrophotometer reader) [44]. The intensity of the color was directly proportional to the number of pro-oxidants present and the antioxidants status of the cell. Briefly, for evaluating TOS status 500 µl of reactive 1 was added to 75 µl plasma (cells supernatant) and absorbance was measured at 530 nm, 25 µl reactive 2 was incorporated in each well and a secondary absorbance was read at 530 nm following a 10 min incubation at room temperature. By using the absorbance values acquired and the following formula, TOS standards were detected in H_2O_2 equivalents/mmol L^{-1} [45,46].

$$TOS = (\Delta\ example/\Delta\ ST2) \times 20$$

Briefly, for evaluating TAC status, 500 µl reactive compound 1 was added to each well followed by the addition of 30 µl of the specimen

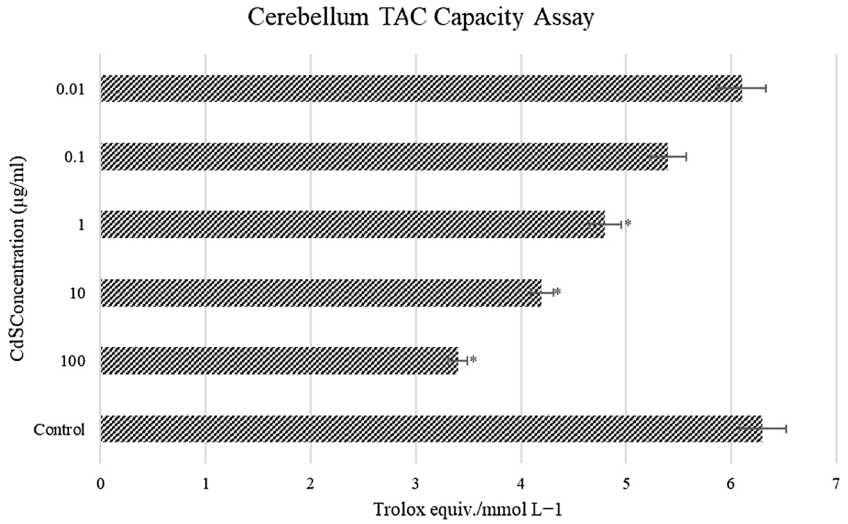

Fig. 5. *In vitro* TAC capacity of CdS (0.01–100 µg/mL) on cerebellum neuron cells (n = 6/group). * Significant differences at $P < 0.05$ compared to control group; ** Significant differences at $P < 0.001$ compared to control group.

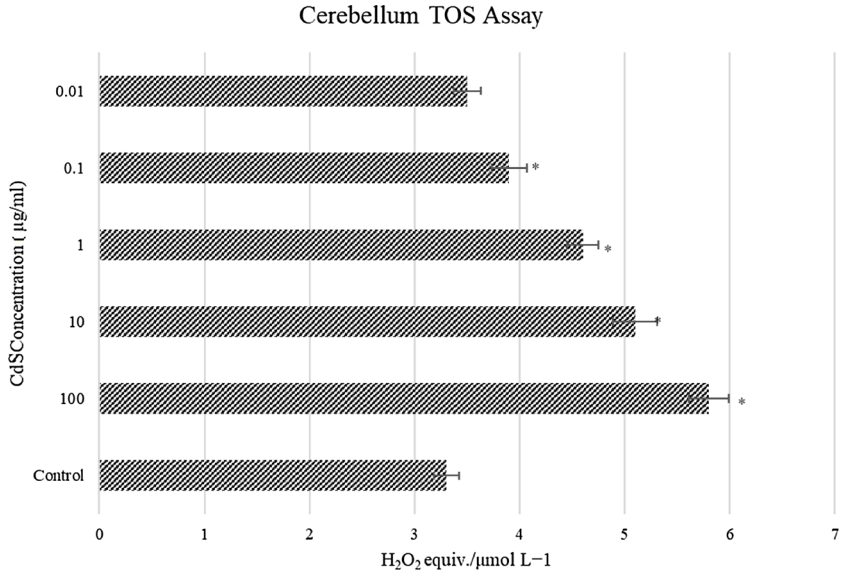

Fig. 6. *In vitro* TOS status of CdS (0.01 – 100 µg/mL) on cerebellum neuron cells (n = 6/group). * Significant differences at $P < 0.05$ compared to control group; ** Significant differences at $P < 0.001$ compared to control group.

and initial absorbance was read at 660 nm (time 0). After the initial reading, 75 µl of reactive 2 was added to the wells, and plates were incubated at room temperature for 10 min. After 10 min, a secondary absorbance value was obtained at 660 nm. While distilled water was used for Standard 1 (blank), Standard 2 in the kit was used as the second point for calibrating the relationship of absorbance intensity to pro-oxidants present. The absorbance values acquired were established according to the following formula, and TAC standards were detected in Trolox™ Equivalents/mmol L^{-1} [47].

TAC = (Δ ST1-Δ example)/(Δ ST1-Δ ST2)

2.2. In vivo study

2.2.1. A rat model for CdS toxicity

Male Sprague-Dawley rats (n = 30) weighing 210 ± 10 g were randomly divided into 6 groups (n = 5/group). Each rat received 1 dose CdS (0, 0.1, 1, 5, 15 or 25 mg/kg) intraperitoneally [48–50]. After 24 h and under deep anesthesia (high dose sevoflurane; Gujarat, İndia), animals were sacrificed by decapitation, and the brain sample was collected (by cutting skull from foramen magna to nose) for pathologic determination.

2.2.2. Ethical approval

This study was conducted at the Medical Experimental Research Center at Ataturk University (Erzurum, Turkey). The Ethical Committee of Ataturk University approved the study protocol (42190979-01-02/2411).

2.2.3. Histopathological determination

Brain tissue was fixed for 48 h in 10 % buffered formaldehyde. The right hemisphere was dehydrated and processed by graded concentrations of alcohol and xylene. Then, immersed in paraffin series and embedded in fresh paraffin. 5 µm sections of whole brain were obtained by using a microtome (Leica, Biosystems, USA). A total of 29 sections (From each 10 obtained section, the first one was used for analysis while the other 9 were discarded; 290 sections in total) were chosen and stained with hematoxylin and eosin (H & E) [51,52].

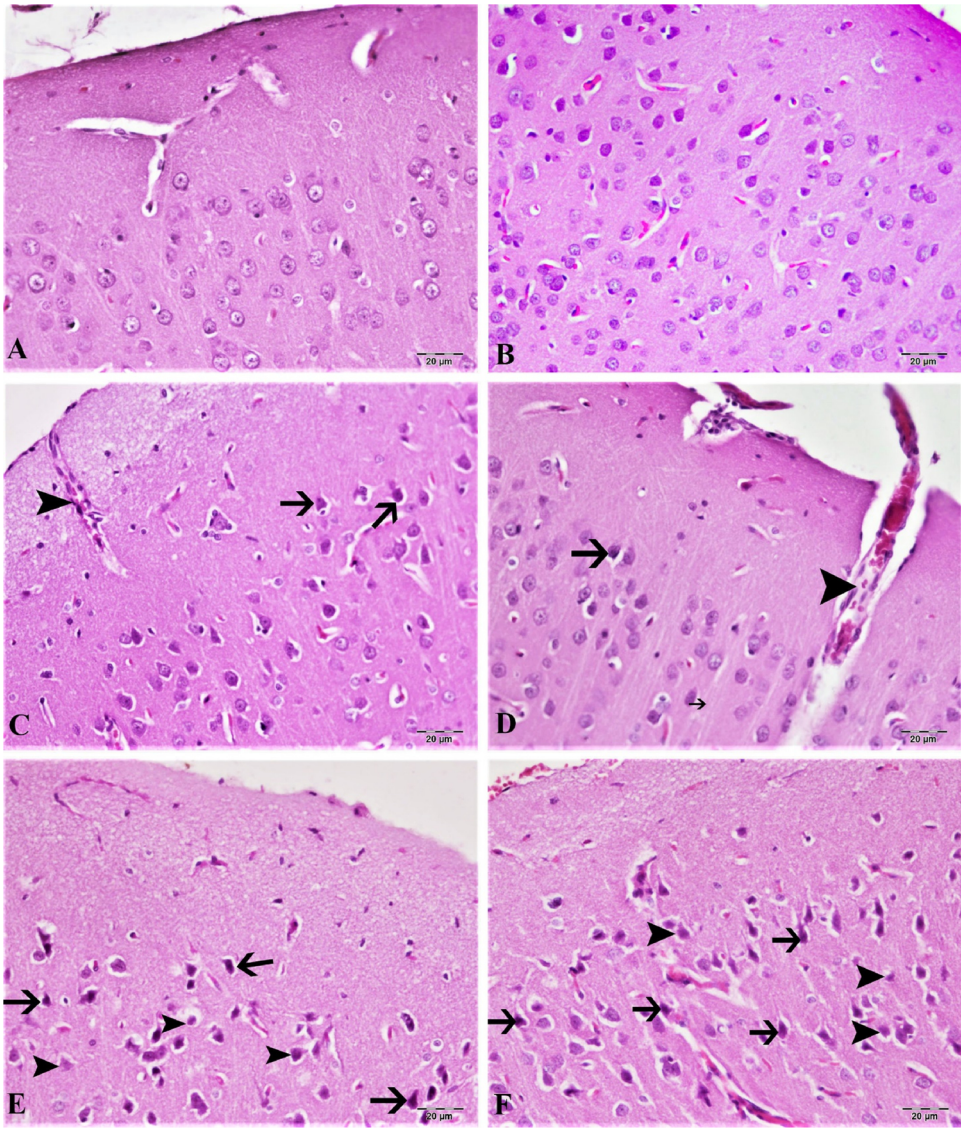

Fig. 7. Brain tissue, (A) control group, normal histological image, (B) 0.1 mg/kg group, mild hyperemia in the vessels, (C) 1 mg/kg group, hyperemia in the vessels, atrophy in very few neurons (arrow), (D) 5 mg/kg groups, severe hyperemia (arrowhead) in the veins, atrophy in the neuron (arrow), (E) 15 mg/kg groups, moderate atrophy in the neurons (arrow), degeneration and necrosis (arrowhead), hyperemia in the vessels, (F) 25 mg/kg groups, Severe hyperemia of the vessels, severe atrophy of neurons (arrow), degeneration and necrosis (arrowhead). H&E, Bar: 20 µm.

2.2.4. Immunohistochemical staining

After dehydration, transparency, and paraffinization, 4–5 µm thick sections were taken from paraffin blocks and placed on Poly-L-lysine slides. Slides were taken into preparation transport apparatus and left at 56 °C for 1 h. Immunohistochemical staining Expose Kit (Abcam: ab80436, UK) was performed as recommended by the manufacturer. Briefly, after xylene and graded ethanol administration, the sample was washed in phosphate buffer (PBS) solution. For blocking endogenous peroxidase activity 10 % hydrogen peroxide was applied. Then protein block (ABCAM: ab80436) was applied to each slide to cover the tissue (block non-specific antibody binding). The primary antibody was re-constituted with 8-OHdG (cat no. Sc66036, dilution 1/50; Santa Cruz, USA) and GFAP (cat no. NB600- 1235, dilution 1/400; Novus Biological, USA). After washing, 1–2 drops of secondary antibody were added for 20 min followed by the addition of horseradish peroxidase (HRP) conjugate. The mixture was incubated for 30 min in a humidified vessel at room temperature. 3 – 3 Diaminobenzidine (DAB) was applied and then washed with distilled water. The hematoxylin (Mayer's) was applied for 15 – 20 sec. The tissue slice was washed until the excess of hematoxylin was removed. After this process, the slides were suspended by lamination with 80 % ethanol, 96 % ethanol, 100 % ethanol, and xylol. Sections were evaluated as (-), mild (+), moderate (++) and severe (+++) according to immune positive values [53].

2.2.5. Statistical analysis

To assess changes following exposure to increasing concentrations of CdS, (concentration-effect), statistical analysis was performed with Kruskal-Wallis and Mann– Whitney *U* test comparisons (IBM SPSS 20.0 software). *P*-value <0.05 was considered as statistically significant.

3. Results

3.1. SEM and EDX analysis

Results from the SEM images (Fig. 2) established that NPs existed in different sizes (8–25 nm, with an average size around 18 nm) and formed clusters. However, it was observed that the clusters which were formed were comprised of NPs of varied sizes that did not exhibit homogeneous distribution. When evaluated based on shape and structure, NPs obtained through biosynthesis were observed both in

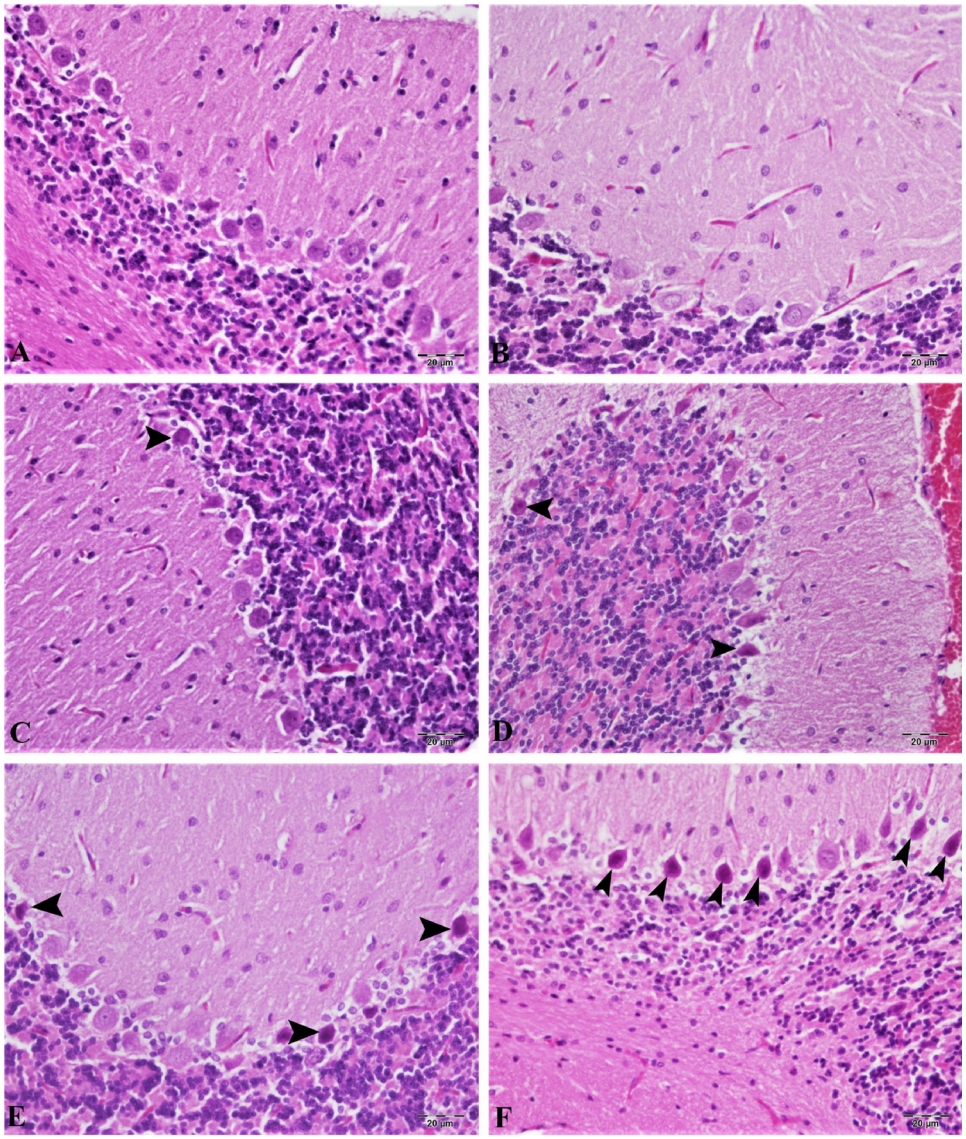

Fig. 8. Cerebral tissue, (A) control group, normal histological image, (B) 0.1 mg/kg group, mild hyperemia in the veins, (C) 1 mg/kg group, atrophy in very few Purkinje cells (arrow), hyperemia in the vessels, (D) 5 mg/kg groups, atrophy in the neuron (arrow), severe hyperemia in the veins, (E) 15 mg/kg groups, moderate atrophy in the neurons (arrow), degeneration and necrosis (arrowhead), hyperemia in the vessels, (F) 25 mg/kg groups, severe hyperemia in the vessels, severe atrophy in neurons (arrow), degeneration and necrosis (arrowhead). H&E, Bar: 20 µm.

spherical and hexagonal structures (Fig. 2).

Corresponding peaks were determined by considering the materials targeted specifically (Cd and S) in the energy-dispersive X-ray (EDX) spectrum. However, different elements are also observed that do not match the Cd or S peak. Unidentified contaminant peaks may arise from the organic structure, which cannot be removed by coating or washing processes for sample analysis (Fig. 3).

3.2. In vitro analyses

3.2.1. Cell Viability, MTT assay

The MTT assay test was performed to determine cellular viability after 24 h of exposure to CdS NPs (Fig. 4). The viability decreased with increasing CdS concentrations. The highest survival rate (93 %) was at the lowest concentration of CdS (0.01 µg/mL), whereas the viability rate at the highest CdS concentration (100 µg/mL) was 56 % ($P < 0.05$) (Fig. 4). Each subsequent concentration yielded further reduced cell viability ($P < 0.05$). The cell viability was decreased slightly in 0.01 µg/mL (minimum of 4%) group, but the maximum decrease was seen in 100 µg/mL (47 %) group compared to the values obtained in the control group.

3.2.2. Total antioxidant capacity (TAC) assay

TAC assay was performed after 24 h exposure to CdS NPs (Fig. 5). The total antioxidant capacity was decreased in a concentration-dependent manner following exposure to CdS. The highest antioxidant rate was seen at the concentration of 0.01 µg/mL CdS (5.2 Trolox™ equivalents/mmol L^{-1}) ($P > 0.05$) and lowest antioxidant capacity was observed at the two highest concentrations of 10 and 100 µg/mL CdS, respectively ($P < 0.05$).

3.2.3. Total oxidant status (TOS) assay

TOS assay was performed following 24 h exposure to CdS NPs (Fig. 6). Total oxidant status was increased following exposure to CdS and this elevation in oxidant status was concentration-dependent ($P < 0.05$). The highest oxidant rate was seen at CdS concentration of 100 µg/mL as determined by changes in the 5.8 H_2O_2 equivalents/mmol L^{-1}. Oxidant status in all concentration groups (except for the

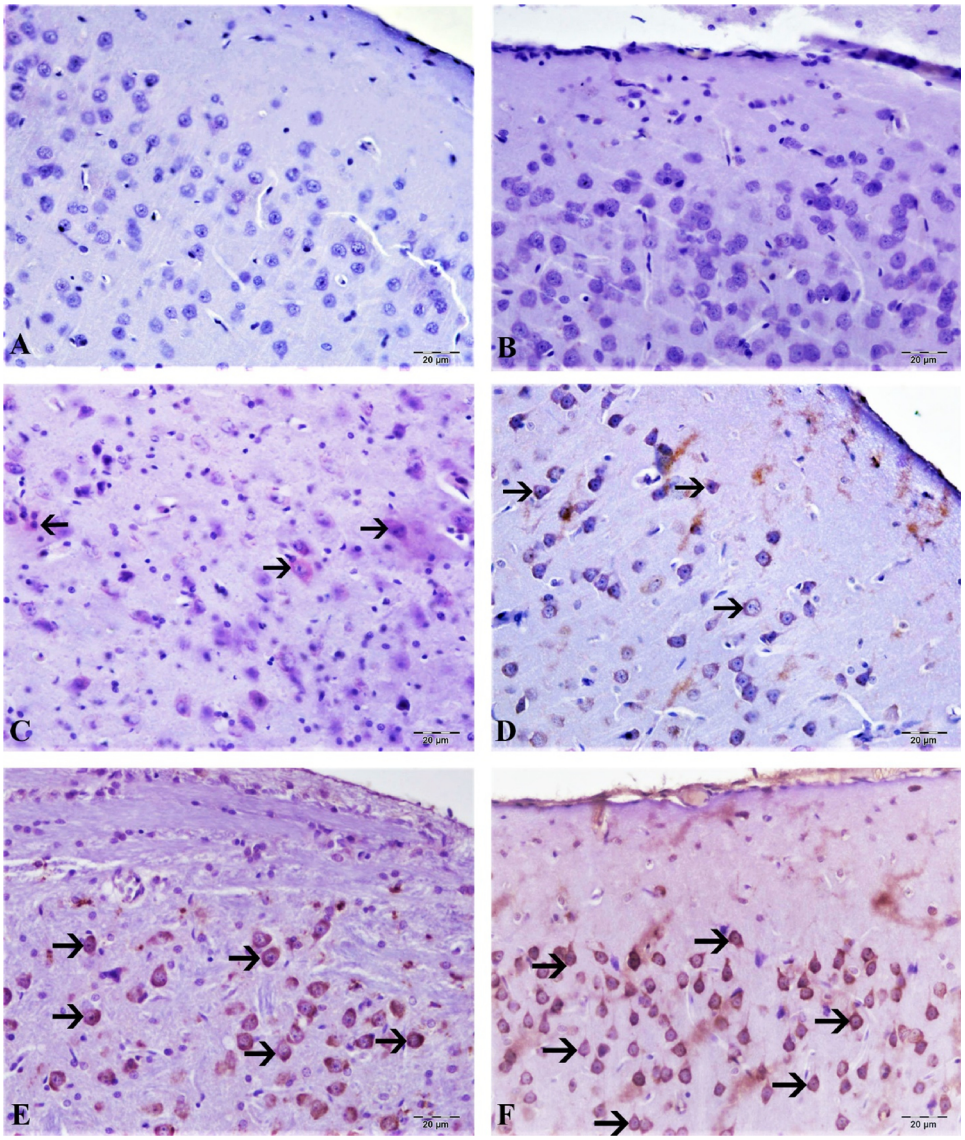

Fig. 9. Brain tissue, (A) control group, 8-OHdG expression is negative, (B) 0.1 mg/kg group, 8- OHdG expression is negative, (C) 1 mg/kg group, very light neurons intracytoplasmic 8-OHdG expression (arrow), (D) 5 mg/kg groups 8 lightweight neurons, 8-OHdG expression (arrow), (E) 15 mg/kg groups, moderate intracytoplasmic expression in neurons 8-OHdG expression (arrow), (F) 25 mg/kg groups, severe intracytoplasmic 8-OHdG expression in neurons (arrow), Bar: 20 µm.

0.01 µg/mL CdS group) was significantly different compared to control group values ($P < 0.05$). The total oxidant status increased from a minimum of 6% (0.01 µg/mL) to a maximum of 75 % (100 µg/mL) compared to the controls.

3.3. In vivo study

3.3.1. Histopathologic determination

Hematoxylin-eosin staining in the cortex and cerebellum are shown in Figs. 7 and 8. According to our results, the control group cortex and cerebellum tissues have normal histological structure (Figs. 7 and 8A). The lowest dose of CdS NPs (0.1 mg/kg) resulted in mild hyperemia in both brain and cerebellum tissues (Figs. 7 and 8B). Increasing the dose of CdS NPs to 1 mg/kg resulted in mild atrophy and degeneration in cortical neurons (Fig. 7C) and Purkinje cells (Fig. 8C). CdS NPs (5 mg/kg) in the cortical neurons showed atrophy, degeneration and hyperemia in the vessels (Fig. 7D). Mild levels of atrophy and degeneration of Purkinje cells in the cerebellum and severe hyperemia in the vessels were noted (Fig. 8D). CdS NPs (15 mg/kg), brain and cerebellum tissues showed moderate degeneration of atrophy in neurons, necrosis and hyperemia in vessels (Fig. 7E). Moderate atrophy and degeneration and liquefaction necrosis were noted in Purkinje cells of the cerebellum (Fig. 8E). At the highest dose of CdS NPs (25 mg/kg), atrophy in the brain was characterized by severe degeneration of neurons, necrosis and hyperemia in the vessels (Figs. 7F; 8 F).

3.3.2. Immunohistochemical determination

8-OHdG and GFAF determination of cortex and cerebellum are shown in Figs. 9–12. No expression of 8-OHdG and Glial fibrillary acidic protein (GFAP) was observed in brain and cerebellum tissue from control animals. CdS NPs (0.1 mg/kg) exposure resulted in increased 8-OHdG expression in the brain and cerebellum tissues, as indicated by expression in neurons and Purkinje cells in the cerebellum. In contrast, minimal GFAP expression was observed in astrocytes. CdS NPs (1 mg/kg) effect on 8-OHdG expression was slight, with detection being observed in very few cortical neurons and Purkinje cells in the cerebellum and only mild GFAP expression was observed in astrocytes. A statistically significant difference ($P < 0.05$) was observed in the CdS NPs (5 mg/kg) group when compared to controls. Intracytoplasmic 8-OHdG expression was observed in a small number of neurons and Purkinje

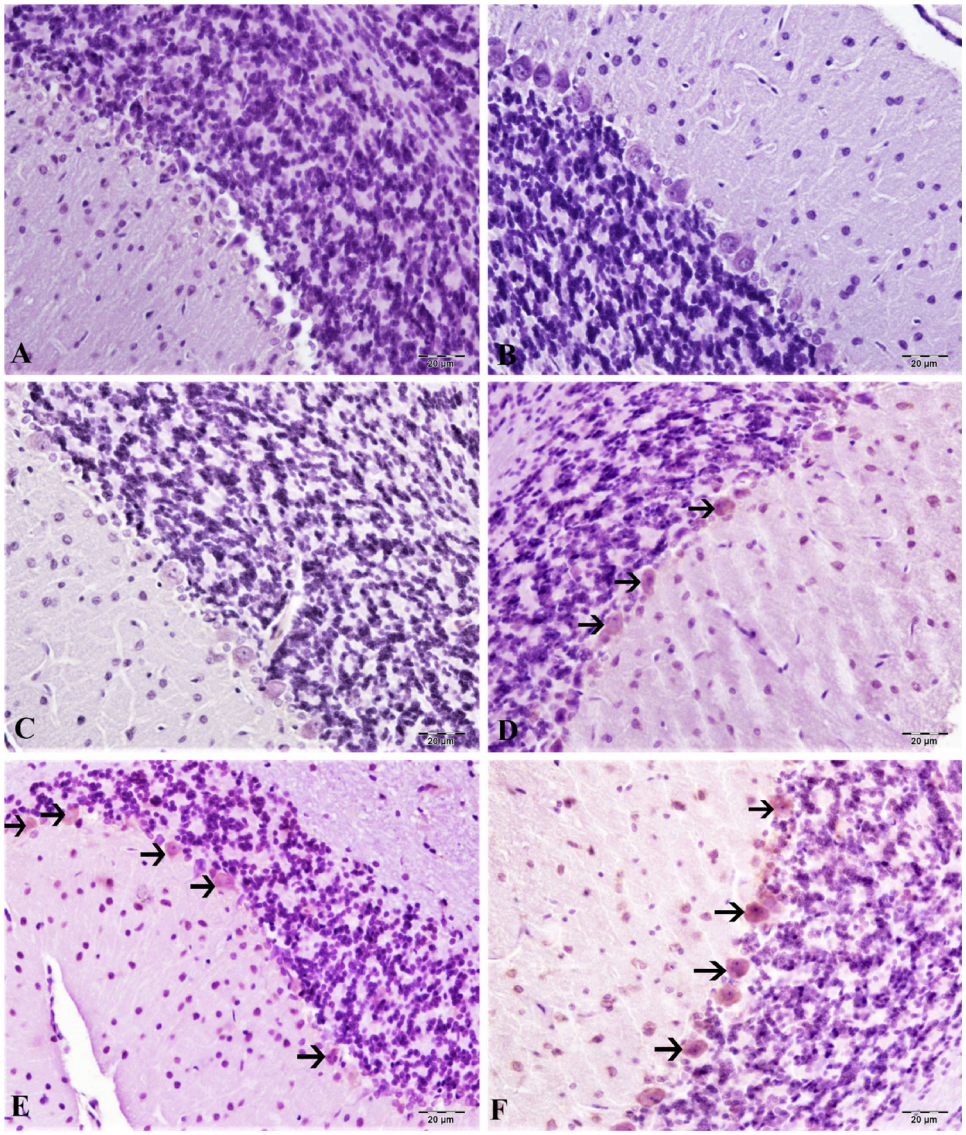

Fig. 10. Cerebral tissue, (A) control group, 8-OHdG expression negative, (B) 0.1 mg/kg group, 8- OHdG expression negative, (C) 1 mg/kg group, 8-OHdG expression negative, (D) 5 mg/kg groups, mild Purkinje cells intracytoplasmic expression of 8-OHdG (arrow), (E) 15 mg/kg groups, moderately intracytoplasmic 8-OHdG expression in Purkinje cells (arrow), (F) 25 mg/kg groups, severe intracytoplasmic 8-OHdG expression in Purkinje cells (arrow), Bar: 20 µm.

cells. There was moderate GFAP expression in astrocytes. When compared to the control group, a statistically significant difference ($P < 0.05$) was observed in the CdS NPs (15 mg/kg) group. Comparing brain and cerebellum tissues, intracytoplasmic 8-OHdG expression was determined to be at a medium level in both neurons and Purkinje cells. There was moderate/severe GFAP expression in astrocytes in the treatment group when compared to the control group ($P < 0.05$). Treatment with CdS NPs (25 mg/kg), comparing brain and cerebellum tissues, intracytoplasmic 8-OHdG expression was detected in a large number of neurons and Purkinje cells. In the brain, very severe GFAP expression was observed in astrocytes. When the CdS NP (25 mg/kg) group was compared to the other treatment groups, the difference was statistically significant ($P < 0.001$).

4. Discussion

We determined the effects of CdS in an *in vitro* toxicity model of cerebellar neuronal cell line and measured cell viability and oxidative stress status with the MTT, TAC and TOS assays. Using SEM imaging and spectrofluorometric analysis, we established the individual dimensions of the particles. Our novel data showed NPs as large clusters (5–8 nm) in size in SEM images. XRD analysis was performed to obtain information on the interplanar spacing and crystal structures of CdS quantum dot nanoparticles synthesized, showing crystal phases in several samples. In general, hexagonal crystals are formed by evaluating the parameters obtained from XRD patterns and evaluating the library and available resources. It graphically shows the crystallite sizes and the band gap ranges obtained from the XRD results. In this study, (002), (101), (110), (201), (004), (314) were obtained by the XRD measurements of CdS obtained by biosynthesis method (27.6°, 31.9°, 45.6°, 54.1°, 56.6°, 66.4° and 75.4°) (203) and (105). The largest peak from the XRD results was measured as the lowest peak width (201) of about 6400 (101) planes. Considering the peak intensity and the output order of the peaks, the structure of the crystals we have obtained approximates a hexagon [54]. We observed several peaks that exhibited intensities suggestive of a shape that ranged from hexagon to cubic structure. When the XRD measured peaks shows our crystals formation are hexagonal [54]. The data from our XRD analysis indicates that the shapes range from spherical to hexagonal. Our XRD results for the CdS quantum point obtained with bacteria have been evaluated as

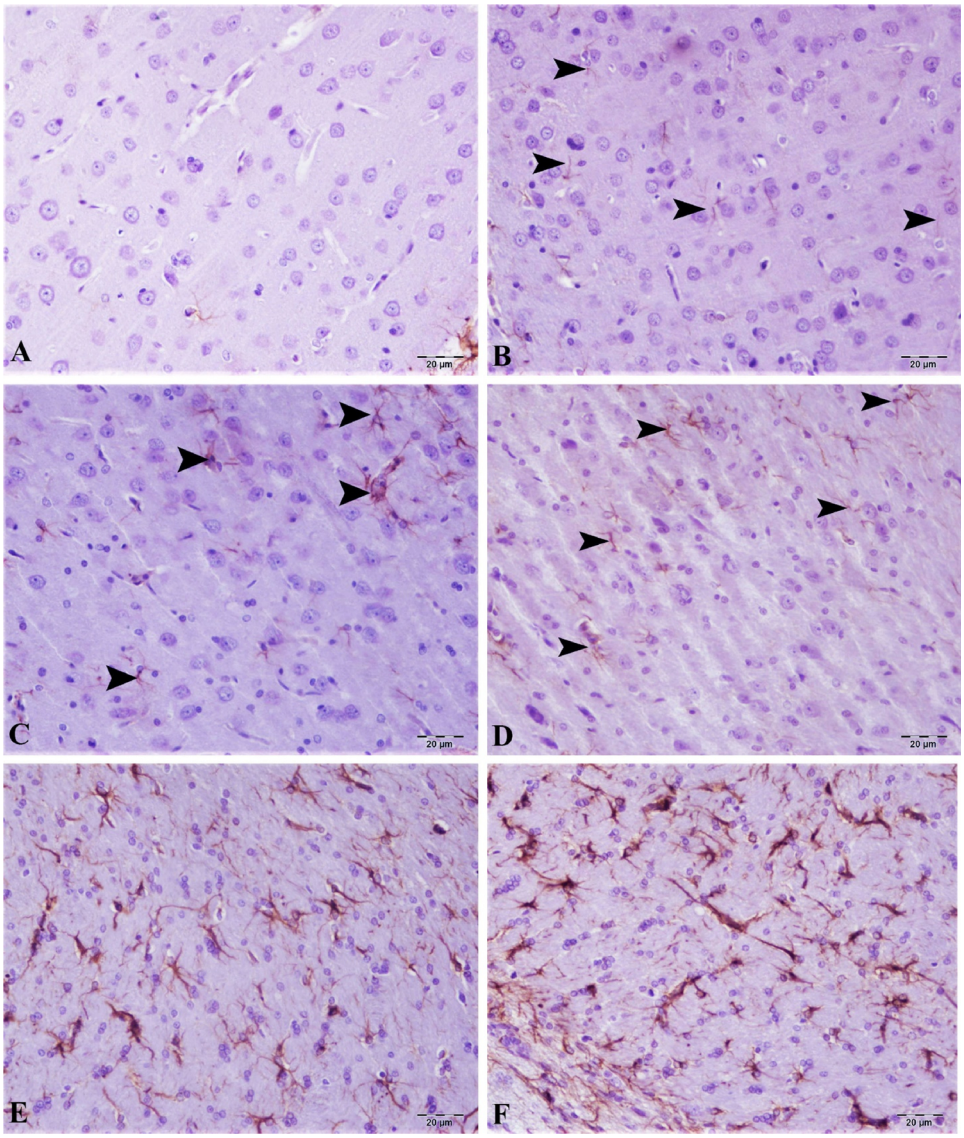

Fig. 11. Brain tissue, (A) control group, GFAP expression was very mild, (B) 0.1 mg/kg group, GFAP expression was very mild, (C) 1 mg/kg group, GFAP expression was mild (arrow), (D) 5 mg/kg groups, GFAP at the intermediate level, (E) 15 mg/kg groups, moderate/severe GFAP expression (arrow), (F) 25 mg/kg groups, severe GFAP expression (arrow), Bar: 20 µm.

hexagonal crystal structures according to the available sources. Diao et al. [27], CdS particle size is essential for determining toxicity. Nanoparticles of 110–130 nm and 80–100 nm CdS were used for investigation of liver tissue toxicity [27]. Their data demonstrated an inverse relationship between size and toxicity with the smaller NPs eliciting greater oxidative damage. In our studies, we used ultra-small CdS nanoparticles, but 0.01 µg/mL failed to show significant toxicity.

According to Nisha et al. [55] surface modification is one of the simplest and most practical techniques to decrease CdS toxicity [55]. In their studies, polyvinylpyrrolidone (PVP) and cysteine were used to cover the nanoparticle surface and evaluate toxicity with Vero cells. The results from these toxicity assay demonstrated that NPs that were surface-coated were less toxic than comparable NPs that were not. The impact of the surface coating was evident by the significantly higher viability for the surface-modified CdS NPs than the unmodified CdS NPs. This data is important since the Li et al. (2018) study present fundamental differences compared to ours (decreased size increased toxicity) but Nisha et al. [55] supported the hypothesis that surface modification can significantly reduce CdS particle toxicity. According to Li and his colleagues CdS toxicity (10 mg/kg for both CdS groups in mice) among 80–100 nm and 110–130 nm were apparent in 80–100 nm group in comparison to the large particle size group. The author stated that in the smaller particle size group, Cd concentration in blood and liver tissue were higher and tissue damage was higher than in large particle size group. Figs. 8, 10 and 12 show necrotic degeneration and DNA fragmentation in neurons and astrocytes in cortical regions, especially with the high CdS NPs doses. Purkinje cells (Figs. 9–11), show distinct pathological signs characterized by degeneration and apoptosis as well as reduced number and smaller cell size compared to the normal control group.

Munari et al., compared 10 nmol/l with 3, 10 nmol/l for 3 and 5 days, 10 and 50 nmol/l for 3, 5, and 7 days in SAOS, HEK293 T and TOLEDO cells, respectively [56,57]. Examining their results, their viability rate is equivalent to that of the control group, and CdS is nontoxic at a concentration of 10 nmol/l. Converting the units of their concentration to match our study, their results correlate with our findings at the lower concentration of NP2 (0.01 µg/mL). However, since they did not perform tests at 50 nmol/l, it is not possible to compare the remainder of their findings with ours.

Pujalte and colleagues used CdS NPs at different concentrations using IP15 (glomerular mesangial) and HK-2 (epithelial proximal) cells

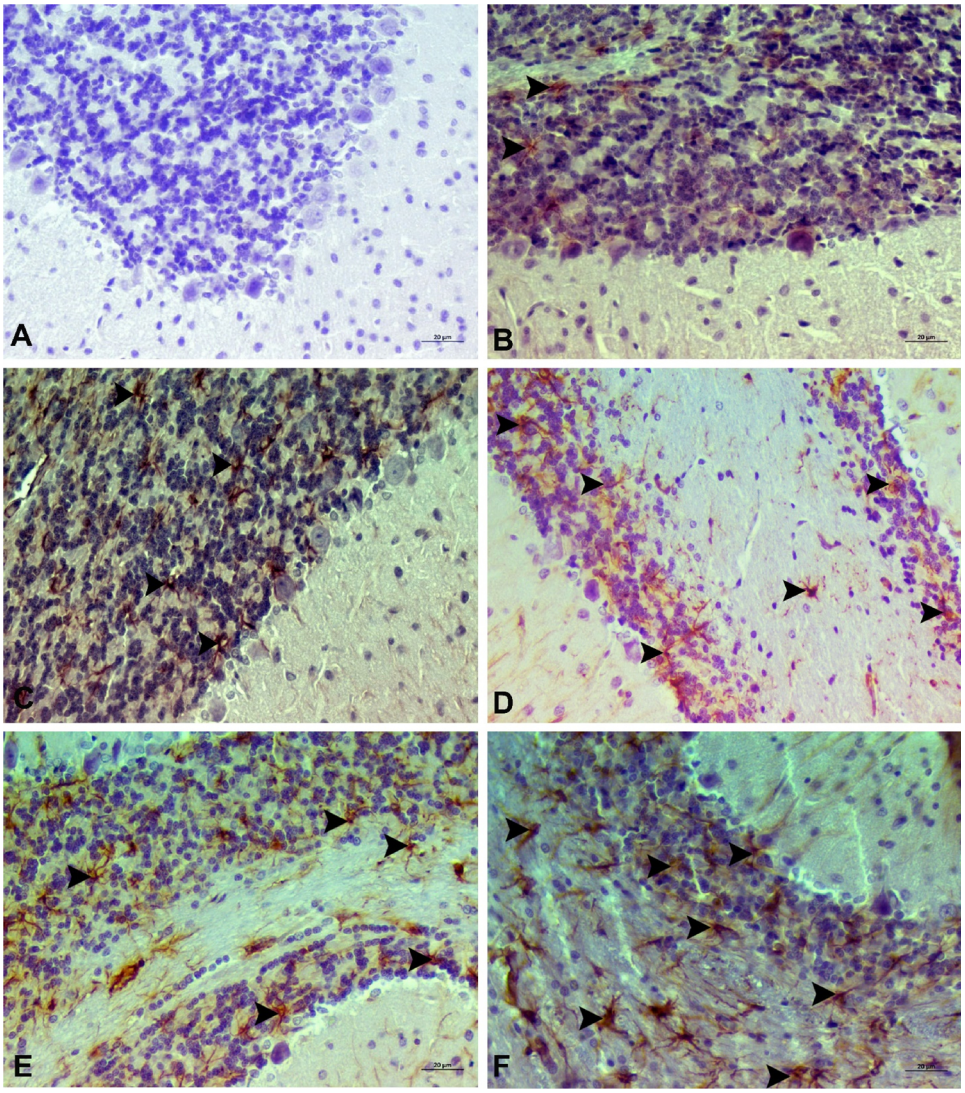

Fig. 12. Cerebellum tissue, (A) control group, GFAP expression is very mild, (B) 0,1 g, GFAP expression is very mild, (C) 1 group, GFAP expression is mild (arrowhead), (D) 5 groups, GFAP expression at intermediate level (arrowhead), (E) 15 groups, moderate/severe GFAP expression (arrowhead), (F) 25 groups, severe GFAP expression (arrowhead), H&E, Bar: 20 µm.

[58]. They noted NPs toxicity at concentrations of 5 µg/cm2 and 6.5 µg/cm2, with no toxicity observed at 1.4 µg/cm2 CdS. Their maximum toxicity at the highest concentration resulted in cell viability of 26 ± 2.5 %. While these results are similar to ours, the concentrations of 0.01 and 0.1 µg/ml did not reveal significant toxicity, but the viability ratio at concentrations of 5 µg/cm2 and 6.5 µg/cm2 showed greater toxicity compared to our results. The variations in the data reported here and in the Pujalte et al. [58] study differ likely due to differing production techniques, overall particle size, or cell type.

Previous reports have suggested that QDs enter the CNS *via* the BBB after systemic redistribution [59]. Jorge Reyes-Esparza and colleague used different dextrin-coated Cd nanoparticles (CdS-Dx/QDs) for one week [60]. They found a high level of fluorescence in kidney, liver and brain and these studies confirmed the effective cellular uptake and even distribution pattern of CdS-Dx/QDs in tissues. In our study, we found all dose of CdS crossed BBB, and in high doses, 8-OHdG and GFAP expression were significantly increased. Pathological findings of our *in vivo* study have confirmed neuronal CdS uptake. Astrocytes have shown higher GFAP expression with increasing CdS dose while in neurons 8-OHdG expression was observed. The IHC staining of neurons and Purkinje cells corroborated that CdS NPs crossed the BBB in-dose dependent manner and induced degeneration and inflammation.

5. Conclusion

The study showed that these NPs may be utilized in biological systems as a delivery agent, or a diagnostic tool provided that the concentration is below the threshold of toxicity (0.01 µg/mL). Our results show that 0.01 µg/mL CdS did not exert significant toxicity in any of the assays performed. Thus CdS NPs should be considered for drug delivery and diagnosis. Nonetheless, additional studies to evaluate the effects of chronic CdS exposure in laboratory animals are warranted. The *in vivo* study revealed that CdS can easily cross the BBB in dose-dependent manner, with signs of degeneration being present only at doses exceeding 0.1 mg/kg.

Declaration of Competing Interest

No potential conflict of interest was reported by the authors.

Acknowledgments

This research did not receive any specific grant from funding agencies in the public, commercial, or not-for-profit sectors. MA was partially supported by grants from the NIEHSR01ES07331 and

R01ES10563. D.R.W was partially supported by Oklahoma State University grant #154357.

Appendix A. Supplementary data

Supplementary material related to this article can be found, in the online version, at doi:https://doi.org/10.1016/j.toxrep.2020.04.011.

References

[1] A.B. Engin, D. Nikitovic, M. Neagu, P. Henrich-Noack, A.O. Docea, M.I. Shtilman, K. Golokhvast, A.M. Tsatsakis, Mechanistic understanding of nanoparticles' interactions with extracellular matrix: the cell and immune system, Part. Fibre Toxicol. (2017) 14.

[2] A. Taghizadehghalehjoughi, A. Hacimuftuoglu, M. Cetin, A.B. Ugur, B. Galateanu, Y. Mezhuev, U. Okkay, N. Taspinar, M. Taspinar, A. Uyanik, B. Gundogdu, M. Mohammadzadeh, K.A. Nalci, P. Stivaktakis, A. Tsatsakis, T.W. Jung, J.H. Jeong, A.M. Abd El-Aty, Effect of metformin/irinotecan-loaded poly-lactic-co-glycolic acid nanoparticles on glioblastoma: in vitro and in vivo studies, Nanomedicine 13 (2018) 1595–1606.

[3] W.T. Huang, Y.P. Ko, T.Y. Kuo, M. Larsson, M.C. Chang, R.D. Jean, D.M. Liu, A new type of gadodiamide-conjugated amphiphilic chitosan nanoparticle and its use for MR imaging with significantly enhanced contrastability, Carbohydr. Polym. 203 (2019) 256–264.

[4] Q. Zeng, D. Shao, et al., The nanotoxicity investigation of optical nanoparticles to cultured cells in vitro, Toxicol. Rep. 1 (2014) 137–144.

[5] Y. Ji, Y. Zhou, et al., Jointed toxicity of TiO_2 NPs and Cd to rice seedlings: NPs alleviated Cd toxicity and Cd promoted NPs uptake, Plant Physiol. Biochem. 110 (2017) 82–93.

[6] M.G. Marosfoi, N. Korin, M.J. Gounis, O. Uzun, S. Vedantham, E.T. Langan, A.L. Papa, O.W. Brooks, C. Johnson, A.S. Puri, D. Bhatta, M. Kanapathipillai, B.R. Bronstein, J.Y. Chueh, D.E. Ingber, A.K. Wakhloo, Shear-activated nanoparticle aggregates combined with temporary endovascular bypass to treat large vessel occlusion, Stroke 46 (2015) 3507–3513.

[7] Abbas Jafarizad, Mehdi Jaymand, Ali Taghizadehghalehjougi, Saeed Mohammadi-Nasr, Amir Mohammad Jabbari, The magnetic graphene-based nanocomposite: an efficient anticancer delivery system, AIP Conf. Proc. (2018) 020039AIP Publishing.

[8] G.C. Lv, K. Li, L. Qiu, Y. Peng, X.Y. Zhao, X. Li, Q.Z. Liu, S.S. Wang, J.G. Lin, Enhanced tumor diagnostic and therapeutic effect of mesoporous silica nanoparticle-mediated pre-targeted strategy, Pharm. Res. (2018) 35.

[9] Marina P. Sutunkova, Larisa I. Privalova, Ilzira A. Minigalieva, Vladimir B. Gurvich, Vladimir G. Panov, A. Boris, The most important inferences from the Ekaterinburg nanotoxicology team's animal experiments assessing adverse health effects of metallic and metal oxide nanoparticles, J. Toxicol. Rep. Katsnelson 5 (2018) 363–376.

[10] S. Kwon, C.H. Cho, et al., Automated measurement of multiple cancer biomarkers using quantum-dot-based microfluidic immunohistochemistry, Anal. Chem. 87 (8) (2015) 4177–4183.

[11] X. Valentini, P. Deneufbourg, et al., Morphological alterations induced by the exposure to TiO_2 nanoparticles in primary cortical neuron cultures and in the brain of rats, Toxicol. Rep. 5 (2018) 878–889.

[12] M.N. Rana, J. Tangpong, et al., Toxicodynamics of lead, cadmium, mercury and arsenic- induced kidney toxicity and treatment strategy: a mini review, Toxicol. Rep. 5 (2018) 704–713.

[13] V. Karri, M. Schuhmacher, et al., Heavy metals (Pb, Cd, As and MeHg) as risk factors for cognitive dysfunction: a general review of metal mixture mechanism in brain, Environ. Toxicol. Pharmacol. 48 (2016) 203–213.

[14] J.M.R. Antoine, L.A.H. Fung, et al., Assessment of the potential health risks associated with the aluminium, arsenic, cadmium and lead content in selected fruits and vegetables grown in Jamaica, Toxicol. Rep. 4 (2017) 181–187.

[15] E.A. Renieri, D.G. Sfakianakis, et al., Nonlinear responses to waterborne cadmium exposure in zebrafish. An in vivo study, Environ. Res. 157 (2017) 173–181.

[16] V. Di Nica, S. Villa, et al., Toxicity of individual pharmaceuticals and their mixtures to Aliivibrio fischeri: evidence of toxicological interactions in binary combinations, Environ. Toxicol. Chem. 36 (3) (2017) 815–822.

[17] A. Buha, R. Jugdaohsingh, et al., Bone mineral health is sensitively related to environmental cadmium exposure- experimental and human data, Environ. Res. 176 (2019) 108539.

[18] V.R. Djordjevic, D.R. Wallace, et al., Environmental cadmium exposure and pancreatic cancer: evidence from case control, animal and in vitro studies, Environ. Int. 128 (2019) 353–361.

[19] D.V. Nica, G.A. Draghici, et al., Short-term effects of very low dose cadmium feeding on copper, manganese and iron homeostasis: a gastropod perspective, Environ. Toxicol. Pharmacol. 65 (2019) 9–13.

[20] P. Modlitbova, K. Novotny, P. Porizka, J. Klus, P. Lubal, H. Zlamalova-Gargosova, J. Kaiser, Comparative investigation of toxicity and bioaccumulation of Cd-based quantum dots and Cd salt in freshwater plant Lemna minor L, Ecotoxicol. Environ. Saf. 147 (2018) 334–341.

[21] K.G. Li, J.T. Chen, S.S. Bai, X. Wen, S.Y. Song, Q. Yu, J. Li, Y.Q. Wang, Intracellular oxidative stress and cadmium ions release induce cytotoxicity of unmodified cadmium sulfide quantum dots, Toxicol. In Vitro 23 (2009) 1007–1013.

[22] N.A. Littefield, B.S. Hass, S.J. James, L.A. Poirier, Protective effect of magnesium on DNA strand breaks induced by nickel or cadmium, Cell Biol. Toxicol. 10 (1994) 127–135.

[23] C. Shi, G. Zhou, Y. Zhu, Y. Su, T. Cheng, H.E. Zhau, L.W.K. Chung, Quantum dots-based multiplexed immunohistochemistry of protein expression in human prostate cancer cells, Eur. J. Histochem. 52 (2008) 127–133.

[24] M.S. Attia, H. Zoulghena, M.S. Abdel-Mottaleb, A new nano-optical sensor thin film cadmium sulfide doped in sol-gel matrix for assessment of alpha-amylase activity in human saliva, Analyst 139 (2014) 793–800.

[25] A.M. Darwish, W.H. Eisa, A.A. Shabaka, M.H. Talaat, Investigation of factors affecting the synthesis of nano-cadmium sulfide by pulsed laser ablation in liquid environment, Spectrochim. Acta A. Mol. Biomol. Spectrosc. 153 (2016) 315–320.

[26] S. Miltonprabu, Nazimabashir, V. Manoharan, Hepatoprotective effect of grape seed proanthocyanidins on Cadmium-induced hepatic injury in rats: possible involvement of mitochondrial dysfunction, inflammation and apoptosis, Toxicol. Rep. 3 (2016) 63–77.

[27] H. Diao, T. Li, R. Zhang, Y. Kang, W. Liu, Y. Cui, S. Wei, N. Wang, L. Li, H. Wang, W. Niu, T. Sun, Facile and green synthesis of fluorescent carbon dots with tunable emission for sensors and cells imaging, Spectrochim. Acta A. Mol. Biomol. Spectrosc. 200 (2018) 226–234.

[28] Bokka Durga, Shaik Raziya, S.G. Rajmahanti, Boddeti Govindh, Korimella Vijaya Raju, Nowduri Annapurna, Synthesis and characterization of cadmium sulphide nanoparticles using annona muricata leaf extract as reducing/capping agent, J. Chem. Sci. Trans. 5 (2016) 1035–1041.

[29] B. Srinivasa Goud, Y. Suresh, S. Annapurna, A.K. Singh, G. Bhikshamaiah, Green synthesis and characterization of cadmium sulphide nanoparticles, Mater. Today Proc. 3 (2016) 4003–4008.

[30] Cherif Ensibi, Mohamed Nejib Daly Yahia, Toxicity assessment of cadmium chloride on planktonic copepods Centropages ponticus using biochemical markers, Toxicol. Rep. 4 (2017) 83–88.

[31] S.J. Iravani, Bacteria in Nanoparticle Synthesis: Current Status and Future Prospects, (2014).

[32] M.O. Kadry, R.M. Abdel-Megeed, et al., Crosstalk between GSK-3, c-Fos, NFκB and TNF-α signaling pathways play an ambitious role in chitosan nanoparticles cancer therapy, Toxicol. Rep. 5 (2018) 723–727.

[33] S. Santra, H. Yang, J.T. Stanley, P.H. Holloway, B.M. Moudgil, G. Walter, R.A. Mericle, Rapid and effective labeling of brain tissue using TAT-conjugated CdS: Mn/ZnS quantum dots, Chem. Commun. (2005) 3144–3146.

[34] T. Siegal, F. Soti, et al., Effect of a chemical delivery system for dexamethasone (Dex-CDS) on peritumoral edema in an experimental brain tumor model, Pharm. Res. 14 (5) (1997) 672–675.

[35] O.M. Abd El-Moneim, A.H. Abd El-Rahim, et al., Evaluation of selenium nanoparticles and doxorubicin effect against hepatocellular carcinoma rat model cytogenetic toxicity and DNA damage, Toxicol. Rep. 5 (2018) 771–776.

[36] F. Stocchi, The therapeutic concept of continuous dopaminergic stimulation (CDS) in the treatment of Parkinson's disease, Parkinsonism Relat. Disord. 15 (Suppl. 3) (2009) S68–71.

[37] V. Garcia-Escudero, R. Gargini, P. Martin-Maestro, E. Garcia, R. Garcia-Escudero, J. Avila, Tau mRNA 3'UTR-to-CDS ratio is increased in Alzheimer disease, Neurosci. Lett. 655 (2017) 101–108.

[38] P.S. Pimprikar, S.S. Joshi, A.R. Kumar, S.S. Zinjarde, S.K. Kulkarni, Influence of biomass and gold salt concentration on nanoparticle synthesis by the tropical marine yeast Yarrowia lipolytica NCIM 3589, Colloids Surf. B-Biointerfaces 74 (2009) 309–316.

[39] M.M.A. El-Raheem, H.M. Ali, Crystallization kinetics determination of Pb15Ge27Se58 chalcogenide glass by using the various heating rates (VHR) method, J. Non-Cryst. Solids 356 (2010) 77–82.

[40] T. Okamura, N. Akai, M. Nakata, Reversible photoisomerization among triplet amino naphthylnitrene, triplet diimine biradical, and indazole: matrix isolation IR spectra of 8-amino-1-naphthylnitrene, 1,8-naphthalenediimine, and 1,2-dihydrobenz[cd]indazole, J. Phys. Chem. A 121 (2017) 1634–1638.

[41] X.H. Wang, Z.W. Nie, L.Y. He, Q. Wang, X.F. Sheng, Isolation of As-tolerant bacteria and their potentials of reducing As and Cd accumulation of edible tissues of vegetables in metal(loid)-contaminated soils, Sci. Total Environ. 579 (2017) 179–189.

[42] J.F. Shao, M. Fujii-Kashino, N. Yamaji, S. Fukuoka, R.F. Shen, J.F. Ma, Isolation and characterization of a rice line with high Cd accumulation for potential use in phytoremediation, Plant Soil 410 (2017) 357–368.

[43] R.Y. Sweeney, C. Mao, X. Gao, J.L. Burt, A.M. Belcher, G. Georgiou, B.L. Iverson, Bacterial biosynthesis of cadmium sulfide nanocrystals, Chem. Biol. 11 (2004) 1553–1559.

[44] A.B.U. Kaplan, M. Cetin, et al., Formulation and in vitro evaluation of topical nanoemulsion and nanoemulsion-based gels containing daidzein, J. Drug Deliv. Sci. Technol. 52 (2019) 189–203.

[45] H. Kamalak, A. Kamalak, A. Taghizadehghalehjoughi, Cytotoxic effects of new-generation bulk-fill composites on human dental pulp stem cells, Cell. Mol. Biol. (Noisy-le-grand) 64 (2018) 62–71.

[46] A. Taghizadehghalehjoughi, M.E. Naldan, Is ketamine suitable for use in glutamate toxicity conditions?: An in vitro study, J. Invest. Surg. (2019) 1–8.

[47] H. Kamalak, A. Kamalak, A. Taghizadehghalehjoughi, A. Hacimuftuoglu, K.A. Nalci, Cytotoxic and biological effects of bulk fill composites on rat cortical neuron cells, Odontology 106 (2018) 377–388.

[48] T. Zhang, Y. Hu, et al., Liver toxicity of cadmium telluride quantum dots (CdTe QDs) due to oxidative stress in vitro and in vivo, Int. J. Mol. Sci. 16 (10) (2015) 23279–23299.

[49] E. Yaghini, H. Turner, et al., In vivo biodistribution and toxicology studies of cadmium-free indium-based quantum dot nanoparticles in a rat model, Nanomedicine 14 (8) (2018) 2644–2655.

[50] D.G. Zayed, S.M. Ebrahim, et al., Combining hydrophilic chemotherapy and hydrophobic phytotherapy via tumor-targeted albumin-QDs nano-hybrids: covalent

coupling and phospholipid complexation approaches, J. Nanobiotechnol. 17 (1) (2019) 7.
[51] C. Sevim, E. Dogan, et al., Tissue-protective effects of French maritime pine bark (Pycnogenol) on glutamate-induced cytotoxicity in adult human dermal fibroblasts, Toxicol. Lett. 280 (2017) S159–S159.
[52] S. Comakli, C. Sevim, et al., Acute glufosinate-based herbicide treatment in rats leads to increased ocular interleukin-1 beta and c-Fos protein levels, as well as intraocular pressure, Toxicol. Rep. 6 (2019) 155–160.
[53] C. Sevim, S. Comakli, et al., An imazamox-based herbicide causes apoptotic changes in rat liver and pancreas, Toxicol. Rep. 6 (2019) 42–50.
[54] N. Soltani, E. Gharibshahi, E. Saion, Band gap of cubic and hexagonal Cds quantum dots – experimental and theoretical studies, Chalcogenide Lett. 9 (2012) 321–328.
[55] K.D. Nisha, M. Navaneethan, B. Dhanalakshmi, K.S. Murali, Y. Hayakawa, S. Ponnusamy, C. Muthamizhchelvan, P. Gunasekaran, Effect of organic-ligands on the toxicity profiles of CdS nanoparticles and functional properties, Colloids Surf. B-Biointerfaces 126 (2015) 407–413.
[56] M. Munari, J. Sturve, G. Frenzilli, M.B. Sanders, A. Brunelli, A. Marcomini, M. Nigro, B.P. Lyons, Genotoxic effects of CdS quantum dots and Ag2S nanoparticles in fish cell lines (RTG-2), Mutat. Res. Genetic Toxicol. Environ. Mutagen. 775 (2014) 89–93.
[57] M. Munari, J. Sturve, G. Frenzilli, M.B. Sanders, P. Christian, M. Nigro, B.P. Lyons, Genotoxic effects of Ag2S and CdS nanoparticles in blue mussel (Mytilus edulis) haemocytes, Chem. Ecol. 30 (2014) 719–725.
[58] I. Pujalte, I. Passagne, B. Brouillaud, M. Treguer, E. Durand, C. Ohayon-Courtes, B. L'Azou, Cytotoxicity and oxidative stress induced by different metallic nanoparticles on human kidney cells, Part. Fibre Toxicol. (2011) 8.
[59] F.A. Cupaioli, F.A. Zucca, D. Boraschi, L. Zecca, Engineered nanoparticles. How brain friendly is this new guest? Prog. Neurobiol. 119–120 (2014) 20–38.
[60] J. Reyes-Esparza, A. Martinez-Mena, I. Gutierrez-Sancha, P. Rodriguez-Fragoso, G.G. de la Cruz, R. Mondragon, L. Rodriguez-Fragoso, Synthesis, characterization and biocompatibility of cadmium sulfide nanoparticles capped with dextrin for in vivo and in vitro imaging application, J. Nanobiotechnol. 13 (2015) 83.